

Reinforcement of polyethylene with polypropylene by a blending and deformation process

EDWARD S. SHERMAN*

Department of Chemical Engineering, Technion – Israel Institute of Technology, Technion City, Haifa, Israel

The blending of polymers to achieve either unique or intermediate properties has become a rather common practice. High density polyethylene (HDPE) and isotactic polypropylene (PP) are immiscible in the melt state and phase segregate. This behaviour and their difference in melting point (~ 132 against $\sim 165^\circ\text{C}$) has been exploited to produce a uniaxial reinforcement of HDPE with PP fibres by a process of melt blending, and tensile drawing followed by annealing. Tensile drawing of the blends results in the transformation of each phase to a fibrous structure having an increased modulus and tensile strength. The annealing of this material to melt and recrystallize the HDPE converts it to a lower modulus ductile lamellar structure which is reinforced with the fibrous PP regions. Both the modulus and tensile strength in the fibre direction fit simple composite theory for isotropic HDPE filled with higher modulus PP fibres over the entire composition range.

1. Introduction

The blending of polymers has become a rather common practice to obtain properties that are either unique or intermediate between those of the blend components. The general scope of this field has been well reviewed in several texts, notably those of Paul and Newman [1] and Manson and Sperling [2].

The structure and properties of blends of polyethylene (PE) and polypropylene (PP) have received considerable attention since they are two of the most commonly used thermoplastics and are of considerable commercial interest in impact modified PP, which is frequently a blend PP, ethylene-propylene rubber and high density polyethylene (HDPE) [3].

This study demonstrates a new concept of utilizing blending and solid state deformation to produce a uniaxial composite of HDPE reinforced with isotactic PP fibres. HDPE and PP are molecularly incompatible [4, 5]. Intensive mixing can result in a fine scale phase segregation with micrometre and submicrometre size domains [6]. Blends of highly ductile semicrystalline polyolefins such as

PP and HDPE can be drawn to transform both phases to a fibrous morphology [7, 8]. As expected, this results in the well known improvements in stiffness and strength of each component [9–11]. A reinforced composite structure was produced from such a deformed blend of HDPE and PP by exploiting the differences in the melting point of each polymer ($\sim 132^\circ\text{C}$ for HDPE and $\sim 165^\circ\text{C}$ for PP). Annealing the sample at fixed length (to prevent shrinkage), between the melting points of PE and PP, and subsequent cooling causes the melting and recrystallization of the PE, converting it from a fibrous to lamellar morphology. The resulting product is non-fibrous HDPE reinforced with PP fibres.

In this communication, the structure and tensile properties of the blend are described at each of the three stages of the process: (i) cold drawing of HDPE–PP blends produced by melt extrusion, (ii) the resultant fibrous product, and (iii) the PP fibre reinforced HDPE that results from annealing and recrystallization. The tensile properties of the final product are then compared with those predicted by simple composite theory.

*Present address: Raychem Corporation, 300 Constitution Drive, Menlo Park, CA 94025, USA.

2. Experimental

2.1. Materials

Stafleone high density polyethylene and Montedison s30s polypropylene were melt blended in an extruder at 200°C at PE compositions 0, 20, 35, 50, 65, 80 and 100 wt % with 0.1 wt % Irganox 1076 antioxidant. After grinding the extrusion was repeated to improve mixing. These resins were chosen since that have almost the same melt index, 0.93 and 0.73 g per 10 min respectively, at 200°C. Samples of circular cross-sections were produced by drawing the melt at 8 mm min⁻¹, from the 8.5 mm diameter die of the extruder down to filaments of ~1.0 mm diameter using a take-up roller. These samples will be referred to as "extruded".

2.2. Drawing and mechanical testing

The extruded samples were cold drawn at room temperature under the same conditions for determining their tensile properties using an Instron. The cross-head speed was 5 cm min⁻¹ for a 10 cm gauge length. The tensile moduli were determined from cross-head displacement with a correction for machine stiffness. The draw ratio, λ , was computed with the reduction in cross-sectional area on drawing by the following equation:

$$\lambda = \left(\frac{d_0}{d_f}\right)^2 \quad (1)$$

with d_0 and d_f as the initial and final sample diameters, respectively. The mechanical properties of the extruded, cold drawn and annealed filaments were measured by the same method. The error bars on the curves indicate the extreme values obtained from no less than five specimens.

2.3. Annealing

Cold drawn samples were clamped with fixed ends in an air circulating oven to prevent shrinkage during the thermal treatment. The temperature was slowly raised (~5°C min⁻¹) to 150°C, which was sufficiently high to melt the PE in the fibres without melting the PP. At this point the oven was turned off, opened and ventilated with a fan to quickly cool and recrystallize the PE. These samples will be referred to as recrystallized.

2.4. Scanning electron microscopy (SEM)

Melt extruded samples were prepared for SEM by notching perpendicular to the extrusion direction and then fracturing in air after 5 to 10 min

immersion in liquid nitrogen. The samples were examined at 25 kV accelerating voltage with a JEOL T-200 SEM after sputter coating with gold.

2.5. X-ray diffraction

Wide angle X-ray diffraction patterns were recorded on flat film in the transmission mode with the extrusion/draw direction perpendicular to the beam. CuK α radiation was used with a sample to film distance of 5.0 cm.

3. Results and discussion

Fig. 1 indicates the change in tensile modulus, E , and yield stress, σ_y , as a function of composition for the extruded samples. The dotted line is the rule of mixing behaviour for the modulus [12] while the solid line is a fit to the experimental data. While the sample to sample variation is large the results tend to fall slightly below this ideal limit. The yield stress increases gradually with PP content to that of pure PP.

Mechanical properties of HDPE-PP blends have been investigated by Noel and Carley [13], Nolley

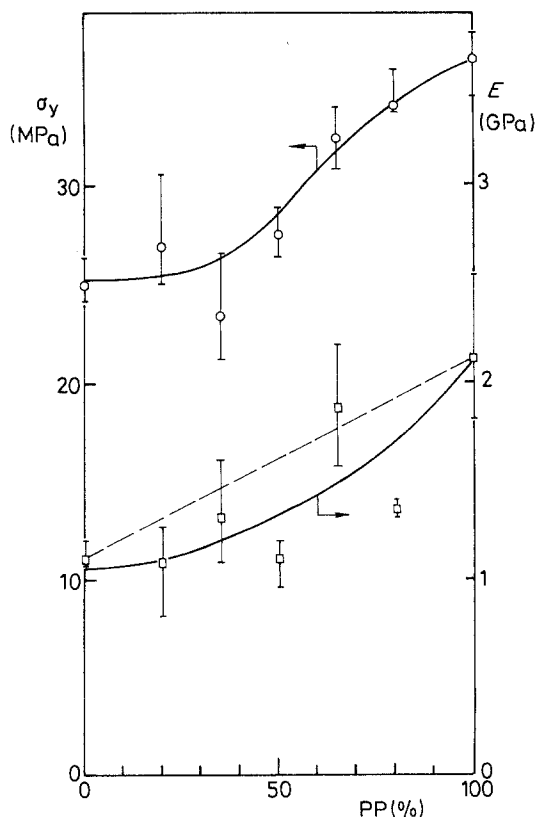


Figure 1 Tensile modulus and yield stress of the extruded blends against composition.

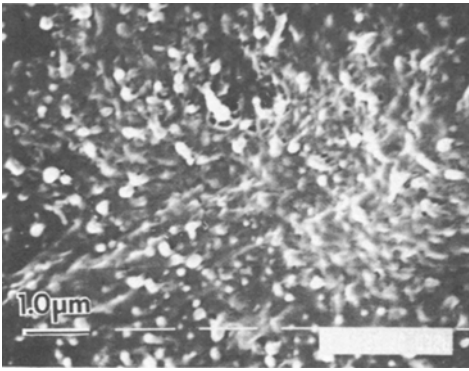


Figure 2 Scanning electron micrograph of the 80% PP extruded sample fracture surface. Spherical HDPE domains ~ 0.1 to $0.25 \mu\text{m}$ in diameter are visible.

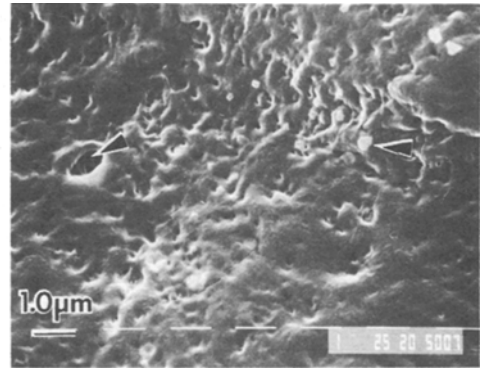


Figure 3 Scanning electron micrograph of the 20% PP extruded sample fracture surface. Holes and sphere $\sim 0.2 \mu\text{m}$ in diameter indicate the dispersion of PP in the HDPE matrix.

et al. [14], Deanin and Sansone [15], Lovinger and Williams [6] and Greco *et al.* [7]. Greco *et al.* have compared and summarized these studies and point out that the behaviour with respect to composition varies greatly due to differences in the molecular weight and melt rheology of the resins as well as the mixing procedure and crystallization conditions. They found that the tensile modulus obeyed the law of mixing while the yield stress showed a positive deviation at approximately 80% PP for their system. Lovinger and Williams [6], however, reported that the yield stress obeyed the law of mixing while the ultimate tensile strength and modulus exhibited a positive deviation from the law of mixing at 75 to 80% PP.

Scanning electron microscopy (SEM) was applied to determine the domain size in each blend composition. Fig. 2 is the brittle fracture surface of the 80% PP sample magnified to show the spherical PE domains which range in diameter from ~ 0.1 to $0.25 \mu\text{m}$. Fig. 3 is from a region of brittle fracture in the 20% PP sample. Both holes from which PP domains detached and those which remained attached to the fracture surface are visible in the figure, as indicated by arrows. The domain size is on the order of $\sim 0.2 \mu\text{m}$. Fracture surfaces of 50/50 composition were very difficult to interpret since the fracture was fairly ductile. The small domains produced and their uniform dispersion at 20% PP and 80% PP suggest good mixing over the entire composition range that should result in a uniform dispersion of fibrillar PE and PP after deformation. This domain size is approximately an order of magnitude better than that achieved by Lovinger and Williams [6] who subjected their blends to 15 min of mixing on a

two roll mill at 200°C . They reported PE domains 2 to $10 \mu\text{m}$ in diameter in 50/50 blends and 1 to $2 \mu\text{m}$ PE domains at 80% PP.

A qualitative description of the crystalline orientation changes in each step of the deformation and annealing process was obtained by X-ray diffraction. Figs. 4a, b and c are the flat film X-ray patterns of the extruded, cold drawn and recrystallized samples, respectively, of 50% PP composition. This sample illustrates the trend observed over the entire composition range. The extruded samples have almost isotropic scattering (continuous rings) for both PE and PP as indicated by the 110, 040 and 121 PP reflections and 110 PE reflection. Highly anisotropic scattering patterns typical of fibrous PE and PP [16, 17] are found after cold drawing. After recrystallization the PP reflections are sharp arcs, indicating the PP crystallites have maintained the orientation present in the cold drawn state. The arcing of 110 PE reflections, however, has increased considerably due to the melting of the oriented PE crystallites.

The tensile testing procedure for the extruded samples produced cold drawn filaments. The natural draw ratio, λ , of these varied with sample composition, as shown in Fig. 5. λ is barely affected by the minor component, remaining close to 8 for PE rich blends against 5.5 for PP rich blends. Only the 50/50 composition had an intermediate value.

The ultimate tensile strength, σ_f , and tensile modulus, E , of the cold drawn filaments are plotted in Fig. 6 as a function of composition. The values of both σ_f and E are nearly identical for the pure PE and PP but vary considerably at inter-

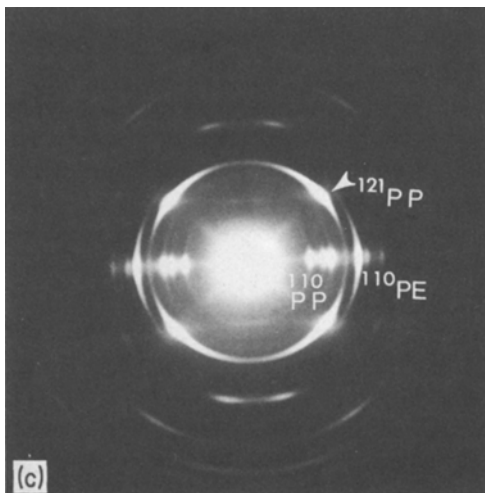
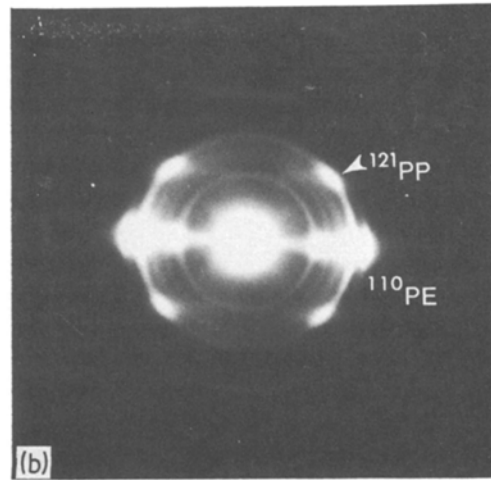
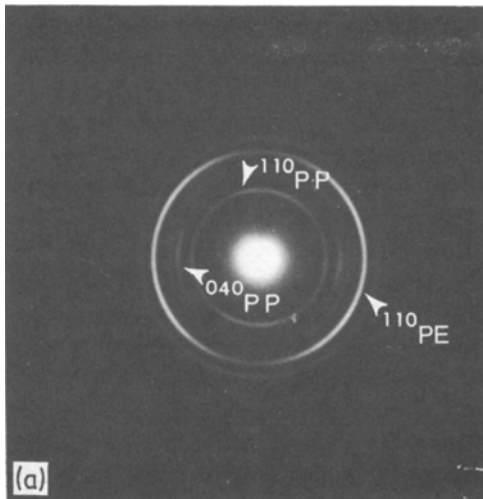


Figure 4 Flat film X-ray diffraction patterns show changes in the crystalline orientation of PP and HDPE in each step of the sample preparation process for 50% PP composition: (a) extruded, (b) cold drawn and (c) annealed sample. The extrusion and drawing directions are vertical.

The strain at failure, ϵ_f , of the cold drawn samples against composition is shown in Fig. 7. An almost linear fit is observed between the low value pure PE and the higher strain of pure PP except for the 65% PP sample which exceeds the strain at failure of even the pure PP significantly. While these results cannot be explained a similar trend in the elongation to break was observed by Greco *et al.* [7] at 60 to 80% PP.

mediate values. Both σ_f and E decrease with the addition of less than 50% PP to PE but then increase for greater than 50% PP compositions. It is impossible to rationalize these data since modulus and strength are a strong function of λ [8, 9], which varies with overall composition (as shown in Fig. 5), and may be different for each phase.

Results from a similar system have been reported by Greco *et al.* [7] in a study of PE-PP blends, drawn at 60° C. They found that deformation at room temperature resulted in failure at low strains such that cold drawn samples could not be produced. They reported a modulus of 12 GPa for pure drawn PE with the modulus of the drawn blends and pure PP between 3.0 and 6.5 GPa. In addition, the tensile strength and elongation at break seemed to be independent of composition.

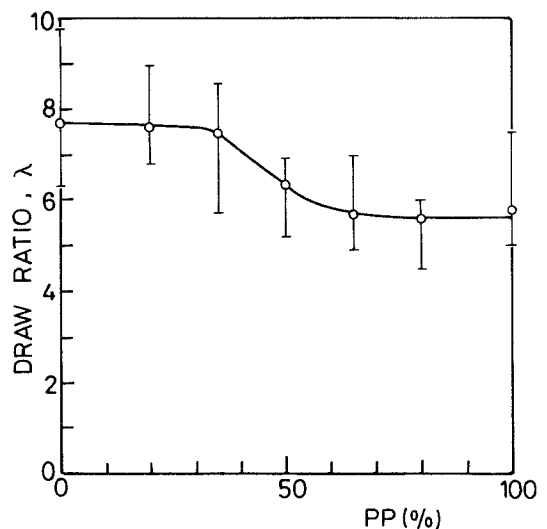


Figure 5 Natural draw ratio which occurred on cold drawing the extruded sample as a function of composition.

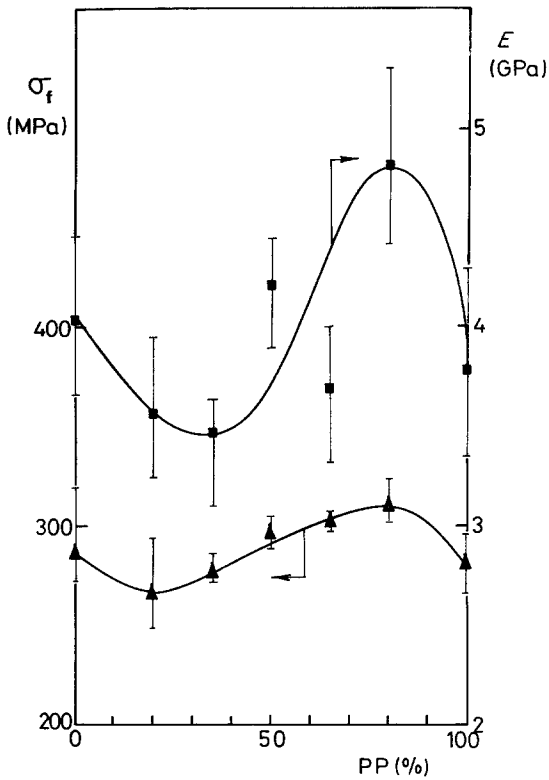


Figure 6 The ultimate tensile strength, σ_f , and tensile modulus, E , of the sample as a function of composition.

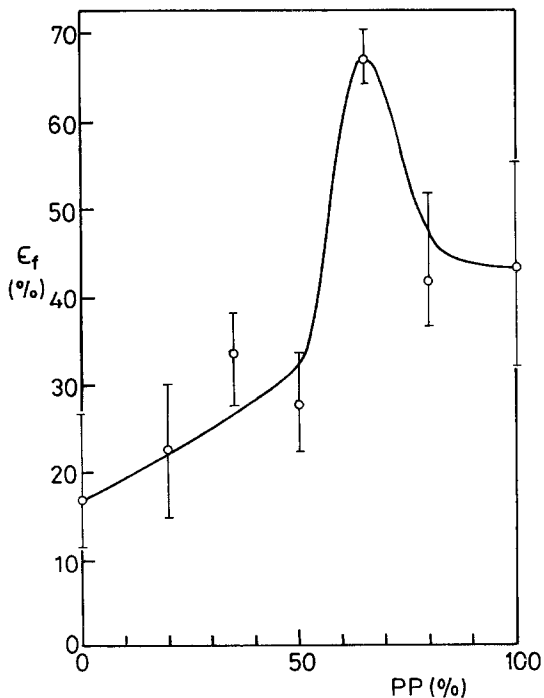


Figure 7 The strain at failure, ϵ_f , of the cold drawn fibres against composition.

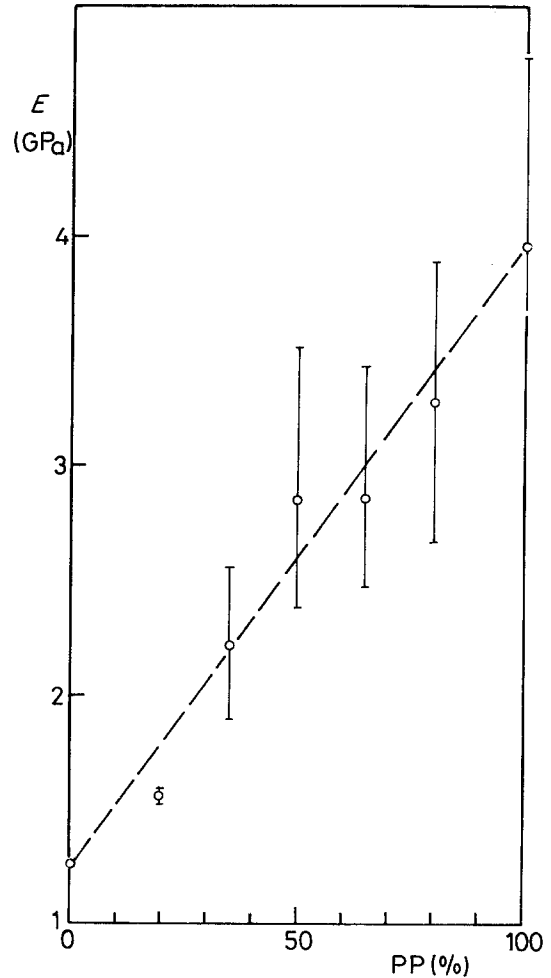


Figure 8 Tensile modulus of the recrystallized samples against composition. The dotted line is the rule of mixing behaviour for equivalent PP fibres in a melt crystallized HDPE matrix.

The tensile modulus of the recrystallized samples as a function of composition is shown in Fig. 8. The modulus of the 100% PE sample is assumed to be equal to that of the extruded sample since it and the PE phase in the recrystallized samples are melt crystallized. The dotted line in the figure is the rule of mixing [12] behaviour:

$$E = E_f V_f + E_m (1 - V_f) \quad (2)$$

where E is the tensile modulus of the composite, E_f is the modulus of recrystallized 100% PP (3.95 GPa), E_m is the modulus of the extruded PE (1.1 GPa) and V_f is the volume fraction of PP, which is present as a fibrous phase. The rule of mixing is applicable for continuous fibres expected for PP compositions greater than 50% (since the

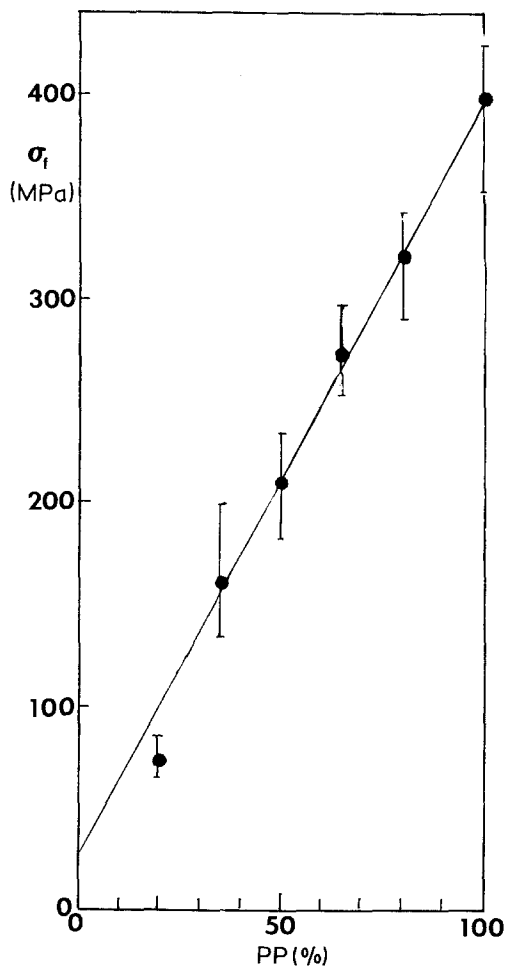


Figure 9 Ultimate tensile strength of the recrystallized samples against composition. The solid line is the theoretical value for continuous fibres in the ductile HDPE matrix.

PP phase is continuous in the extruded material (it should remain continuous after deformation) as well as high aspect ratio non-continuous fibres [18]. The good fit of the ideal behaviour justified the assumption of the E_m value and suggests that the PP fibres are either continuous or greater than the critical aspect ratio at all compositions.

The ultimate tensile strength of the recrystallized samples was also determined and compared with behaviour predicted by composite theory. These results are shown in Fig. 9. No value is assigned to 100% PE composition since its failure would involve yielding, cold drawing of PE and then the failure of the cold drawn fibres. The solid line in the figure is the theoretical value for a continuous fibre reinforced composite with a ductile matrix [19].

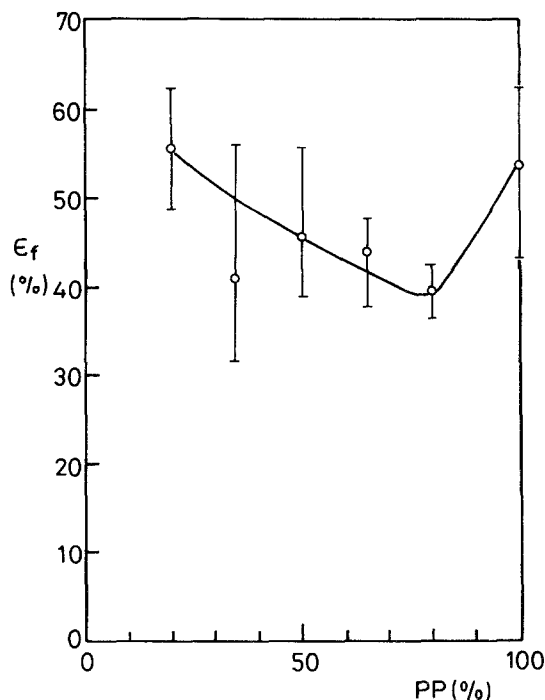


Figure 10 The strain at failure of the recrystallized samples plotted against composition. The solid line is a smooth fit to the experimental data.

$$\sigma_f = \sigma_{\text{fibre}} V_f + (\sigma_m)_{\epsilon_f} (1 - V_f) \quad (3)$$

where σ_f is the ultimate strength of the composite, σ_{fibre} is the ultimate strength of the 100% PP sample after annealing (400 MPa) and $(\sigma_m)_{\epsilon_f}$ is the stress in the pure matrix at the strain at failure of the fibre (ϵ_f , 55%). $(\sigma_m)_{\epsilon_f}$ was determined to be 25 MPa from the stress-strain curve of the extruded pure PE sample. This excellent correspondence of the results with theory demonstrates that a fibrous composite has been created by this process.

The strain at failure, ϵ_f , of the annealed samples as a function of composition is shown in Fig. 10 with the solid line fit to the experimental data. The trend of decreasing elongation with increasing PP fibre volume fraction is evident. The strain of failure of the 80% PP composition is lower than that of the pure PP sample. The decrease in elongation with increasing fibre volume fraction is expected for ductile fibres in a ductile matrix [20]. The greater ductility of the pure PP fibres probably reflects the lower concentration of defects in a homogeneous fibrous material rather than the fibre-fibre composite formed via plastic deformation of the HDPE matrix. The strain at failure of the recrystallized samples is greater than

that of the cold drawn samples except at 65 to 80% PP composition. This can be seen by comparing Figs. 7 and 10.

4. Conclusions

The reinforcement of HDPE with fibrous PP has been achieved via blending, followed by cold drawing and annealing. Melt blending produced a dispersion of 100 to 250 nm diameter domains of the minor component. Cold drawing of this structure then resulted in the formation of two fibrous phases with an increase in tensile modulus.

Annealing the cold drawn samples at fixed length at 150°C followed by cooling resulted in the melting and recrystallization of HDPE. This caused a reduction in the crystalline orientation of the HDPE phase and a loss of its fibrous properties, resulting in an HDPE matrix reinforced with drawn-annealed PP fibres. The modulus and ultimate tensile strength of these filaments agreed with continuous fibre composite theory.

The results demonstrate a unique method of obtaining fibre composite properties from polymer blends. Further investigations of transverse, tear and impact properties are warranted for this and similar systems to define unique polymer-polymer composite properties.

Acknowledgements

The author wishes to acknowledge the financial support of the Lady Davis Foundation as a post-doctoral fellow, which made this work possible. The advice and comments of A. Ram and R. Salovey are also greatly appreciated.

References

1. D. R. PAUL and S. NEWMAN, "Polymer Blends" (Academic Press, New York, 1978).

2. J. A. MANSON and L. N. SPERLING, "Polymer Blends and Composites" (Plenum Press, New York, 1976).
3. J. M. HODGKINSON, A. SAVADORI and J. G. WILLIAMS, *J. Mater. Sci.* **18** (1983) 2319.
4. G. D. WIGNALL, H. R. CHILD and R. J. SAMUELS, *Polymer* **23** (1982) 957.
5. J. L. ZAKIN, R. SIMHU and H. HERSHEY, *J. Appl. Polym. Sci.* **10** (1966) 1455.
6. A. J. LOVINGER and M. L. WILLIAMS, *ibid.* **25** (1980) 1703.
7. R. GRECO, G. MUCCIARIELLO, G. RAGOSTA and E. MARTUSCELLI, *J. Mater. Sci.* **16** (1981) 1001.
8. M. TANG, R. GRECO, G. RAGOSTA and S. CIMMINO, *ibid.* **18** (1983) 1031.
9. W. C. SHEEHAN and T. B. COLE, *J. Appl. Polym. Sci.* **8** (1964) 2359.
10. G. CAPACCIO and I. M. WARD, *Polymer* **15** (1974) 233.
11. R. J. SAMUELS, "Structured Polymer Properties" (John Wiley and Sons, New York, 1974) p. 27.
12. B. D. AGARWAL and L. J. BROUTMAN, "Analysis and Performance of Fiber Composites" (John Wiley and Sons, New York, 1980) p. 22.
13. O. F. NOEL and J. F. CARLEY, *Polym. Eng. Sci.* **15** (1975) 117.
14. E. NOLLEY, J. W. BARLOW and D. R. PAUL, *ibid.* **10** (1980) 364.
15. R. D. DEANIN and M. F. SANSONE, *Polym. Prep. Amer. Chem. Soc., Div. Polym. Chem.* **1** (1) (1978) 211.
16. A. PETERLIN and G. MEINEL, *Makromol. Chem.* **142** (1971) 227.
17. R. J. SAMUELS, *J. Polym. Sci.* **A3** (1965) 1741.
18. B. D. AGARWAL and L. J. BROUTMAN, "Analysis and Performance of Fiber Composites" (John Wiley and Sons, New York, 1980) p. 28.
19. *Idem, ibid.* p. 83.
20. *Idem, ibid.* p. 27.

Received 20 January
and accepted 8 February 1984